SOFT MATERIALS

Structure and Dynamics

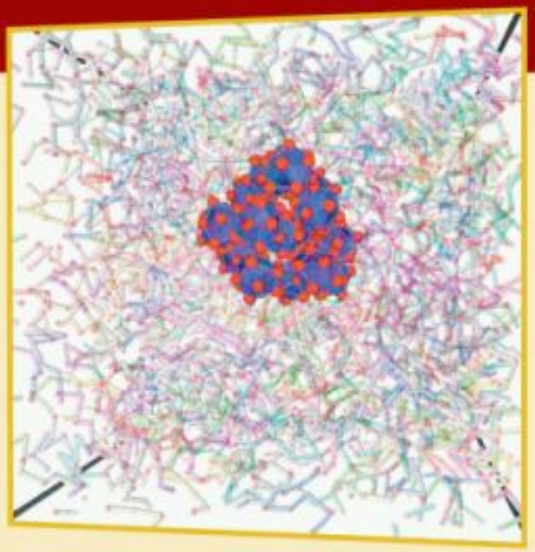

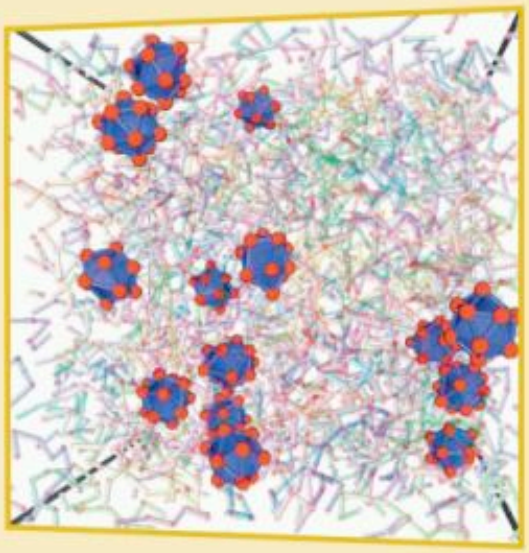

Edited by
John R. Dutcher and
Alejandro G. Marangoni

Science and Engineering of Nanoparticle-Polymer Composites: Insights from Computer Simulation

FRANCIS W. STARR Department of Physics, Wesleyan University, Middletown, Connecticut

SHARON C. GLOTZER Departments of Chemical Engineering and Materials Science and Engineering, University of Michigan, Ann Arbor, Michigan

1 INTRODUCTION

Modification of polymers with an inorganic material to produce a polymer composite is commonplace in the world of modern plastics. Polymer nanocomposites, in which the secondary material has dimensions on nanometer scales, offer exciting opportunities not possible with conventional composites [1–3]. Vast improvements in properties ranging from mechanical [4] to fire resistance [5, 6] can be achieved with small amounts of the nanostructured inorganic additives. As a result, polymer nanocomposites are much lighter than conventional polymer composites, while displaying large increases in tensile modulus, strength, toughness and other bulk properties. Besides their improved properties, polymer nanocomposites are easily molded or extruded, simplifying manufacturing processes. Despite significant progress in materials development, a comprehensive understanding of polymer nanocomposites yielding predictive structure-property relationships is not yet in hand. Without such understanding, progress in nanocomposite development has been largely empirical.

In the last decade, with the explosive development of different kinds of nanoparticles and nanostructured molecules [7–13], such as gold and semi-conductor nanoparticles, carbon nanotubes, Buckeyballs, polyhedral oligomeric silsesquioxanes, etc., many types of polymer nanocomposites have been developed and researched. A common feature in all these hybrid materials, which distinguishes polymer nanocomposites from traditional composites and filled polymers, is the huge interfacial region resulting from the nanoscopic dimensions of the inorganic component. The enormous amount of interface present means that most of the polymers interact directly with the inorganic component, introducing heterogeneity within the polymer matrix on the nanoscale and deforming the polymer from its bulk conformation. In these unique materials, with only a few volume percent of dispersed nanoparticles, the entire polymer matrix may be considered to be a nanoscopically confined polymer [2].

Polymer nanocomposite performance is defined by three major characteristics [2]: the nanoscale inorganic component, the nanoscopically confined matrix polymer, and the arrangement of the inorganic component within the matrix. Generally speaking, the ultimate properties of a nanoparticle-polymer composite depend as much on the individual properties of the organic and inorganic components as on the relative arrangement and interaction between them. Computer simulations offer a unique opportunity to observe nanoscopic and molecular-level structural and dynamical details in model nanocomposites not readily accessible in experiments. In particular, close examination of the behavior of the polymer chains in the direct vicinity of the nanoparticle, the extent to which the nanoparticle affects the local chain structure and dynamics, and the detailed arrangement of nanoparticles and how it is affected by the strength of polymer-particle interactions, shear, etc., can be studied via molecular simulation with coarse-grained interaction potentials. The results of several such studies are reviewed in this chapter [14–16]. We refer the reader to additional computational studies of nanofilled polymers that are not discussed here [17–24].

The chapter is structured as follows. In Section 2, we describe the simulation methodology and model we have used to study basic features of nanoparticle-filled homopolymers. In Section 3, we describe our findings on the effect of a single model nanoparticle on the local structure of the polymer chains, and on the local and bulk dynamics. In Section 4, we discuss what our simulations suggest about the role of interactions on nanoparticle dispersion and the role of particle clustering and dispersion on bulk properties like viscosity, and we discuss the possible physical processes controlling nanoparticle clustering. We conclude with a brief discussion of outstanding questions and challenges in Section 5.

2 SIMULATION

Specific details of the simulations can be found in refs. [14–16]; we outline the details here for completeness. The first series of simulations [14, 15] focused on the structural and dynamic properties of polymer chains in the vicinity of a single polyhedral nanoparticle. The polyhedral shape of the nanoparticle was chosen for its similarity to existing nanoparticles, such as fullerenes and metallic nanoparticles [25, 26]. We also considered this highly symmetric shape because it poses fewer geometrical complications in coding and subsequent analysis than tube- or plate-like nanoparticles (such as carbon nanotubes or organic nanoclays).

Since the goal of these studies was to identify basic physical characteristics of nanoparticle filled polymer melts that are largely independent of the chemical details of the system, we chose to model the system using very simple potentials that capture only the essential features of the system, such as the chain connectivity, chain statistics, and

nanoparticle geometry. Specifically the polymer chains were represented using a common model in which monomers, interacting via Lennard Jones interactions, are bonded to nearest neighbor monomers of the chain via a "FENE" anharmonic spring potential [27–29]. Similarly, the nanoparticle was represented by a collection of Lennard Jones particles, bonded in such a way to roughly maintain the icosahedral geometry of the nanoparticle, but allowing for vibrations of the individual force sites around their ideal locations.

The second series of simulations [16] focused on nanoparticle dispersion and its relation to properties. Building upon the previous simulations, the system was modeled using the same potentials, but a range of nanoparticle loadings (volume fractions) and interactions were considered to determine the relation to nanoparticle clustering.

3 EFFECT OF A SINGLE NANOPARTICLE ON POLYMER PROPERTIES

3.1 Local structure

To investigate the structural changes in the vicinity of the nanoparticle surface, refs. [14, 15] separately examined the behavior of the monomers that make up the chains and the overall behavior of the center-of-mass of the chains. The monomer structure in the vicinity of the nanoparticle was studied using the monomer density $\rho(d)$ as a function of the distance d from the nanoparticle surface. Since the nano-particle is nearly spherical, the calculation is simplified by estimating $d = r - r_{\rm surface}$, where r is the radial position of a monomer relative to the particle center, and $r_{\rm surface} = \frac{1}{12}(42 + 18\sqrt{5})^{\frac{1}{2}}\ell$ is the radius of the inscribed sphere of the icosahedron. We show $\rho(d)$ with (i) attractive and (ii) non-attractive (excluded volume only) interactions between monomers and the nanoparticle in Fig. 1.

Due to simple packing constraints, $\rho(d)$ has a well-defined layer structure in both cases. The primary differences in the density profile occur in the vicinity nearest the nanoparticle surface. In the attractive case, the monomer density in the first layer is enhanced due to the relatively strong monomer-particle attraction. Additionally, the peak location changes only weakly with temperature, since there is a preferred distance due to the attractions between the nanoparticle and the monomers. The splitting in the first peak at lowest T is due to the fact that the nanoparticle is not spherical, and those monomers near the vertices of the nanoparticle are at a slightly larger distance than those near the center of a face of the nanoparticle. In the case of non-attractive interactions, there is also an enhancement in the density in the first layer, but in this case it is attributable to monomers far from the nanoparticle "pressing" the inner monomers toward the interface with the nanoparticle. Moreover, since there is no preferred distance

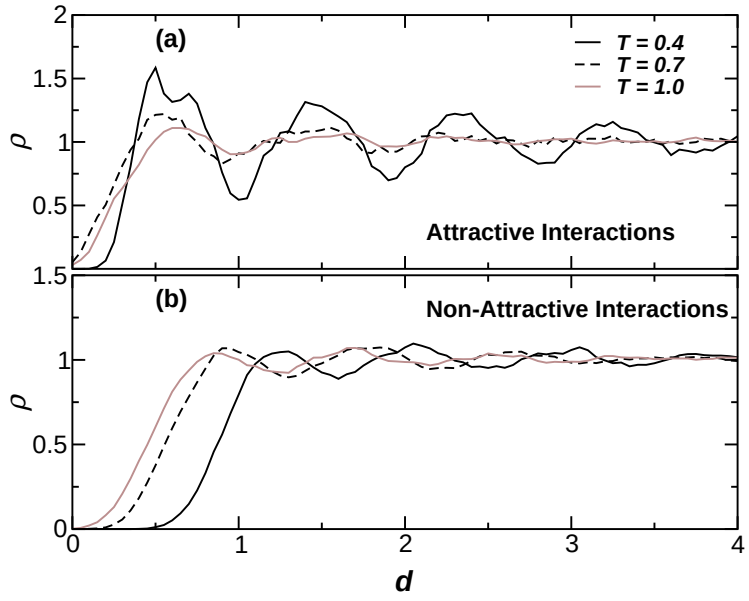

Figure 1: Monomer density profile $\rho(d)$ as a function of the distance from the nano-particle surface at several temperatures for both (a) attractive and (b) non-attractive monomer-particle interactions. [14, 15]

for the inner-most monomers, the location of the first peak is more strongly T dependent. The location of the first peak is slightly larger than in the attractive nanoparticle case, and the position of this peak increases with decreasing T. The presence of a maximum and subsequent oscillations in $\rho(d)$ for both the attractive and non-attractive cases is consistent with the density profile of monomers observed near a smooth wall [30–33].

The local packing of the polymer chains can be quantified by examining the the radius of gyration

$$R_g^2 = \frac{1}{M^2} \left\langle \sum_{i,j=0}^{M} (\mathbf{r}_i - \mathbf{r}_j)^2 \right\rangle , \tag{1}$$

where M is the number of monomers that make up a chain. To be sensitive to interfacial effects, ref. [14] calculated R_g as a function of d, distance of the center-of-mass of a chain from the nanoparticle surface. Furthermore, to gain insight into the orientation of the chains, the radial component $R_g^{\perp}$ of R_g relative to the nanoparticle center was calculated. In so far as the nanoparticle can be approximated by a sphere, $R_g^{\perp}$ is the component perpendicular to the particle surface. The radial component is found by substituting the segment vector $\mathbf{r}_i - \mathbf{r}_j$ in Eq. 1 with the dot product of the segment vector and the

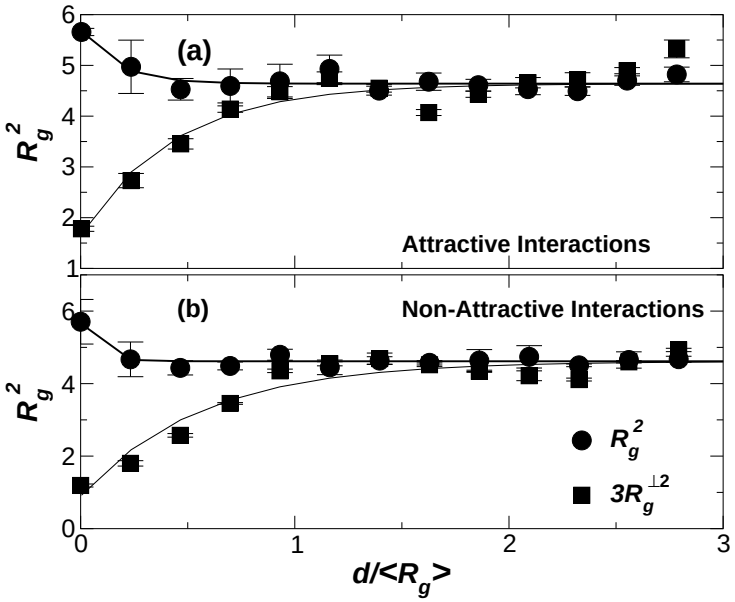

Figure 2: Radius of gyration R_g of the polymer chains as a function of distance $d/\langle R_g \rangle$ of the center of mass of a chain from the nano-particle surface for $T = 0.4$. The component of R_g perpendicular to the surface is labeled by $R_g^{\perp}$. We show results for both (a) attractive and (b) non-attractive interactions. The increase of R_g, coupled with the decrease of $R_g^{\perp}$, indicates that the chains become increasingly elongated and "flattened" as the surface of the nano-particle is approached. The effect appears largely independent of the temperature and numerical values of the potential parameters. [14, 15]

normalized bisector of each chain segment relative to the particle center, yielding

$$R_g^{\perp\,2} = \frac{1}{M^2} \left\langle \sum_{i,j=0}^{N} \left(\frac{(\mathbf{r}_i - \mathbf{r}_j) \cdot (\mathbf{r}_i + \mathbf{r}_j)}{|\mathbf{r}_i + \mathbf{r}_j|} \right)^2 \right\rangle . \tag{2}$$

The behavior of R_g^2 and $R_g^{\perp\,2}$ is nearly identical for both the attractive and non-attractive monomer-nanoparticle interactions (Fig. 2). The independence of the chain structure on the choice of interactions suggests that changes in the structure are primarily due to geometric constraints of packing the chains close to the surface. More specifically, R_g^2 increases by about 25% on approaching the particle surface, while $R_g^{\perp\,2}$ decreases by slightly more than a factor of 2. These results indicate that the polymers become slightly elongated near the surface, and flatten significantly, orienting with the particle surface. At $d \approx R_g$, the chain shape becomes bulk-like. Hence, the surface provides a preferential orientation for the polymers, and it is natural that this effect should persist for a distance

R_g, roughly the chain size. We also point out that this result depends only weakly on T. These results are also reminiscent of the properties of polymers near a wall and polymer thin-films [30–33], despite the fact that the size of the chains is comparable to that of the nanoparticle, meaning that there is significant curvature in the interface on the scale of the polymer chains.

3.2 Local and Bulk Dynamics

To elucidate how the polymer dynamics are influenced by the interactions with the surface, it is necessary to consider the melt dynamics as a function of distance from the nano-particle surface. Single monomer dynamics can be studied though the incoherent, or self scattering function

$$F_{\rm self}(q,t) = \frac{1}{N}\left\langle \sum_{j=1}^{N} e^{-i\mathbf{q}\cdot[\mathbf{r}_j(t)-\mathbf{r}_j(0)]} \right\rangle, \tag{3}$$

where $\mathbf{q}$ the wave vector and $\mathbf{r}_j(t)$ is the location of particle j at time t. $F_{\rm self}(q,t)$ is the Fourier transform of the real-space time-dependent spatial-correlation function. Unfortunately, by this standard definition, $F_{\rm self}(q,t)$ is averaged over the entire system and hence difficult to relate to surface properties.

To probe the surface properties, ref. [15] utilized the fact that monomers form well-defined layers surrounding the nanoparticle (see Fig. 1) and split $F_{\rm self}(q,t)$ into the contribution from monomers located in each layer at $t = 0$. In this way, eq. 3 can be decomposed as

$$F_{\rm self}(q,t) = \frac{1}{N}\sum_{\rm layers} N_{\rm layer} F_{\rm self}^{\rm layer}(q,t), \tag{4}$$

where $N_{\rm layer}$ is the number of monomers in a given layer.

$F_{\rm self}^{\rm layer}(q_0,t)$ is plotted for $T = 0.4$ in Fig. 3. Here q_0 denotes the value of the first peak in the static structure factor $S(q)$. The relaxation of the monomers closest to the nanoparticle surface are slowest when the monomers and nanoparticle have an attractive interaction. Conversely, when there is no attraction between monomers and the nanoparticle, the relaxation of surface layer monomers is significantly enhanced compared to the bulk. The altered dynamics persist for a distance slightly less than $2R_g$ (radius of gyration) from the surface. The systems show a two-step relaxation at this T because the relaxation occurs through a fast vibrational motion and a slower structural rearrangement that occurs on a significantly longer time scale. Fig. 3 also shows the relaxation of $F_{\rm self}(q_0,t)$ for a pure system at the same density and temperature. The results for the pure system nearly coincide with the behavior of the outer-most layer, regardless of the choice of monomer-particle interactions, indicating that at large

Soft Materials: Structure and Dynamics pp. 107-124
Eds.: J. R. Dutcher and A. G. Marangoni (2004)

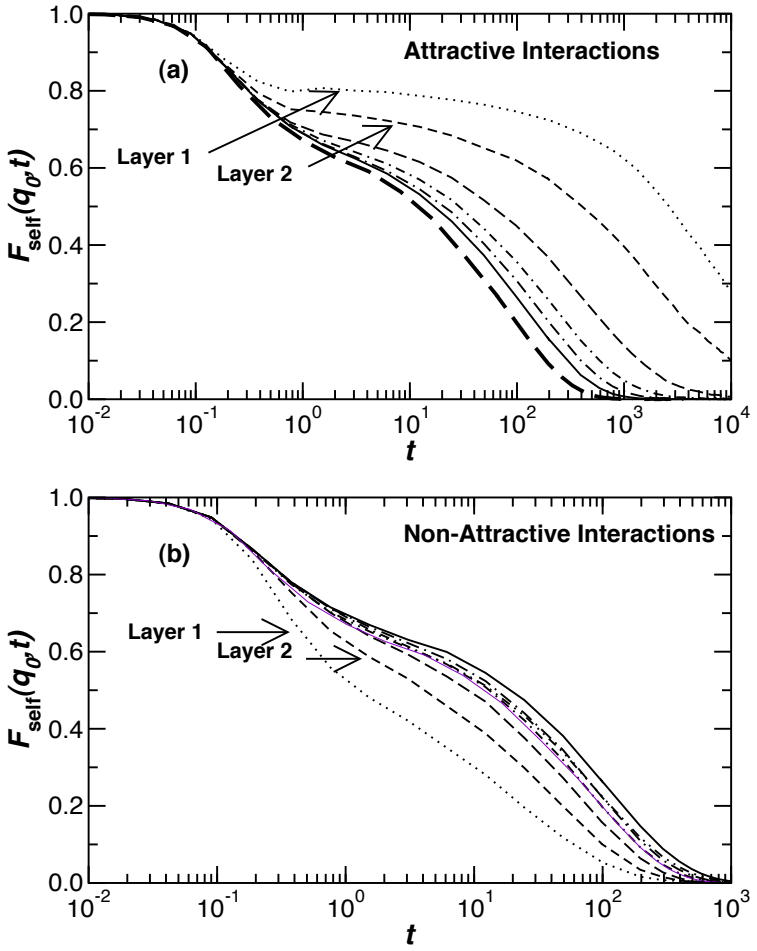

Figure 3: $F_{\rm self}(q_0,t)$ for the average of all monomers (dotted line) and decomposed into layers (defined by the distance from the nano-particle surface) for (a) attractive interactions and (b) non-attractive interactions at $T = 0.4$. Layers are defined using the monomer density profile $\rho(d)$ shown in Fig. 1. The minima in $\rho(d)$ define the boundary between layers. In (a), the relaxation near the nano-particle surface is slowed by roughly 2 orders of magnitude. In contrast, (b) shows the relaxation of $F_{\rm self}(q_0,t)$ is enhanced by roughly one order of magnitude near the surface. The relaxation time of the outer-most layer in both cases nearly coincides with the relaxation time of the pure system. [14, 15]

distances bulk-like behavior is recovered. The impact of the surface roughness on the surface dynamics has also recently been considered [34].

These changes in the local dynamics naturally also have an effect on the overall bulk dynamics of the system. Far from the nanoparticle surface, the dynamics of these systems nearly coincides with those of a pure system, and so the changes in bulk properties depend only on the change in the surface properties. Hence, the system with attractive interactions is expected to have longer average relaxation time, and the system without attraction should have a smaller average relaxation time. This can be clearly illustrated by the relaxation time τ of the spherically averaged intermediate scattering function

$$F(q,t) \equiv \frac{1}{NS(q)} \left\langle \sum_{j,k=1}^{N} e^{-i\mathbf{q}\cdot[\mathbf{r}_k(t)-\mathbf{r}_j(0)]} \right\rangle . \tag{5}$$

$F(q,t)$ is normalized by the structure factor $S(q)$ such that $F(q,0) = 1$. The relaxation time τ is defined by $F(q,\tau) \equiv 0.2$. The exact choice for the definition of τ does not qualitatively affect the results. At each T, τ is larger than that of the pure system for the attractive system, and this difference increases with decreasing T (Fig. 4). Conversely, τ in the non-attractive system is slightly smaller at low T than in the pure system, and this difference increases with decreasing T. These observations can be related to the bulk properties of the system through the glass transition temperature T_g. Given the relative changes in τ, the attractive system is expected to have greater T_g than the pure system, and the non-attractive system should have a T_g less the pure system.

Ref. [14, 15] estimated changes in T_g by fitting τ to the Vogel-Fulcher-Tammann (VFT) form

$$\tau \sim e^{A/(T-T_0)} \tag{6}$$

where T_0 is typically quite close to the experimental T_g value [35], provided the data fit are at sufficiently low T; hence changes in T_g are reflected in T_0. T_0 increases in the system with attractive interactions, but decreases in the system with only an excluded volume interaction. Thus, the effect of the steric hindrance introduced by the nanoparticle decreases $\tau(T)$ and T_0, in spite of the fact that monomers have a reduced number of directions in which to move, and hence degrees of freedom that aid in the loss of correlations. The fact that T_0 shifts in opposite directions for attractive versus purely excluded volume interactions further demonstrates the importance of the surface interactions. Similar results for the bulk viscosity have also been found [21]. Other systems, like thin films [33] and brushes [36] show similar dynamical phenomena.

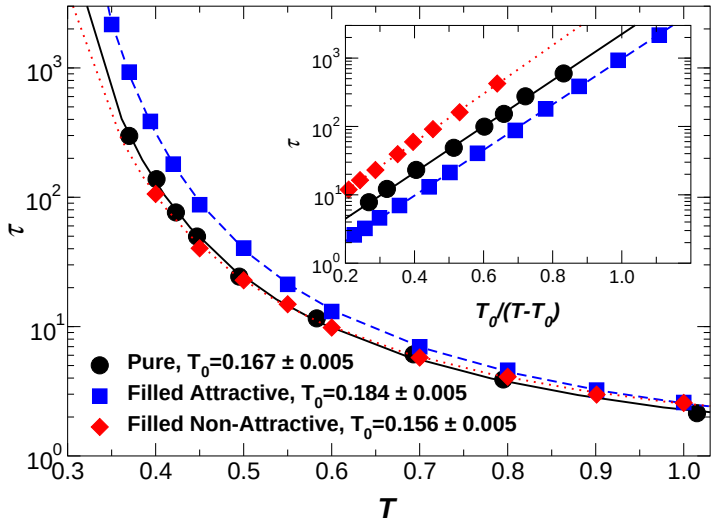

Figure 4: Temperature dependence of the relaxation time of the intermediate scattering function. The lines are a fit to the VFT form of Eq. (6). The inset shows the same data plotted against reduced temperature $T_0/(T - T_0)$ to show the quality of the VFT fit. For clarity in the inset, τ of the pure system is multiplied by 2, and τ of the filled non-attractive system is multiplied by 4. [14, 15]

4 COMPOSITE MATERIALS

4.1 Role of interactions on particle clustering

Nanoparticle clustering can be controlled through a variety of parameters, such as concentration and temperature. One of the most fundamental parameters affecting the tendency of nanoparticles to aggregate or disperse is the interactions between the nanoparticles, and the interactions between nanoparticles and the surrounding polymer matrix. Ref. [16] determined the range of interactions for which clustering or dispersion occurs, and in doing so, provides some insight into the mechanism controlling clustering. In the following, we summarize how varying polymer-nanoparticle interactions while keeping the loading volume fraction of nanoparticles, ϕ, fixed alters the clustering properties of the nanocomposite. Additionally, varying the monomer-particle interaction strength $\varepsilon_{\rm mp}$ and holding T fixed eliminates changes in clustering that arise from simple vibrational excitation. Such vibrational changes can obscure changes in properties due to changes in the state of particle clustering.

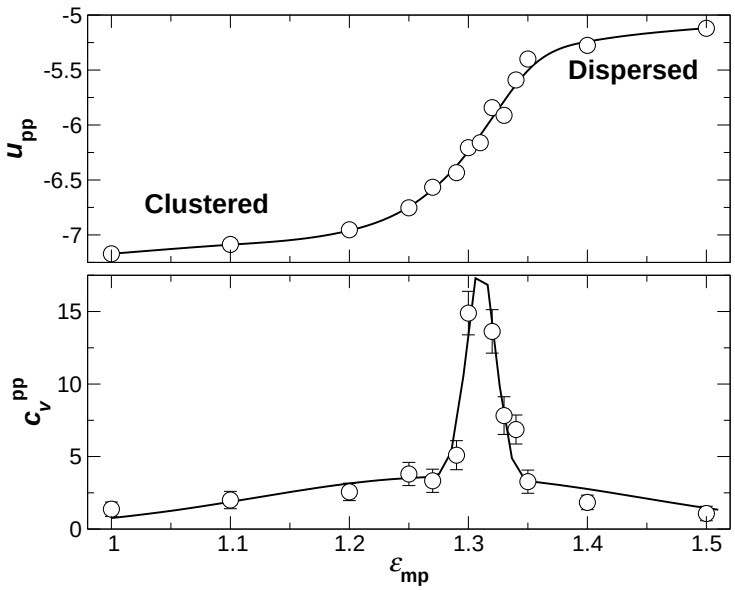

Figure 5: (a) The nanoparticle component of the potential energy $u_{\rm pp}$ shows the crossover between clustered (low $u_{\rm pp}$) and dispersed (high $u_{\rm pp}$) states. Since the T is held constant, changes in $u_{\rm pp}$ are dominated by the clustering of the nanoparticles. (b) The specific heat $c_V^{\rm pp}$ maximum provides a more reliable estimate of the crossover point between clustered and dispersed states. Figure is reproduced from ref. [16].

In order to track changes in nanoparticle clustering, a simple and reliable metric indicating the qualitative changes in clustering is needed. As particles cluster, there are significant changes in the particle-particle and particle-monomer components of the potential energy, reflecting the difference in the number of particle-particle or particle-monomer contacts in the system. Hence ref. [16] used the potential energy per force site between nanoparticles $u_{\rm pp}$ as an indicator of nanoparticle clustering. Additionally, the specific heat $c_V^{\rm pp} = \partial u_{\rm pp}/\partial T$ aids in the identification of the crossover point between the asymptotic limits of clustering and dispersion.

Fig. 5(a) shows $u_{\rm pp}$ as a function of the monomer-particle interaction strength $\varepsilon_{\rm mp}$ at fixed $\phi = 0.094$ and $T = 2.0$. At large and small $\varepsilon_{\rm mp}$, $u_{\rm pp}$ is nearly constant, but makes a relatively abrupt crossover between two extremes over a narrow range $1.25 < \varepsilon_{\rm mp} < 1.35$. Visual inspection of the configurations (Fig. 6) at the extreme values of $\varepsilon_{\rm mp}$ confirms that the low values of $u_{\rm pp}$ correspond to clustered states, while the larger values correspond to dispersed configurations. Hence, for this (T,ϕ), $\varepsilon_{\rm mp}$ needs to be only slightly stronger than $\varepsilon \equiv 1$ (the monomer-monomer interactions) for the particles to disperse. The range over which the crossover occurs is more clearly shown by $c_V^{\rm pp}$ (Fig. 5(b)). Moreover, very

Soft Materials: Structure and Dynamics pp. 107-124
Eds.: J. R. Dutcher and A. G. Marangoni (2004)

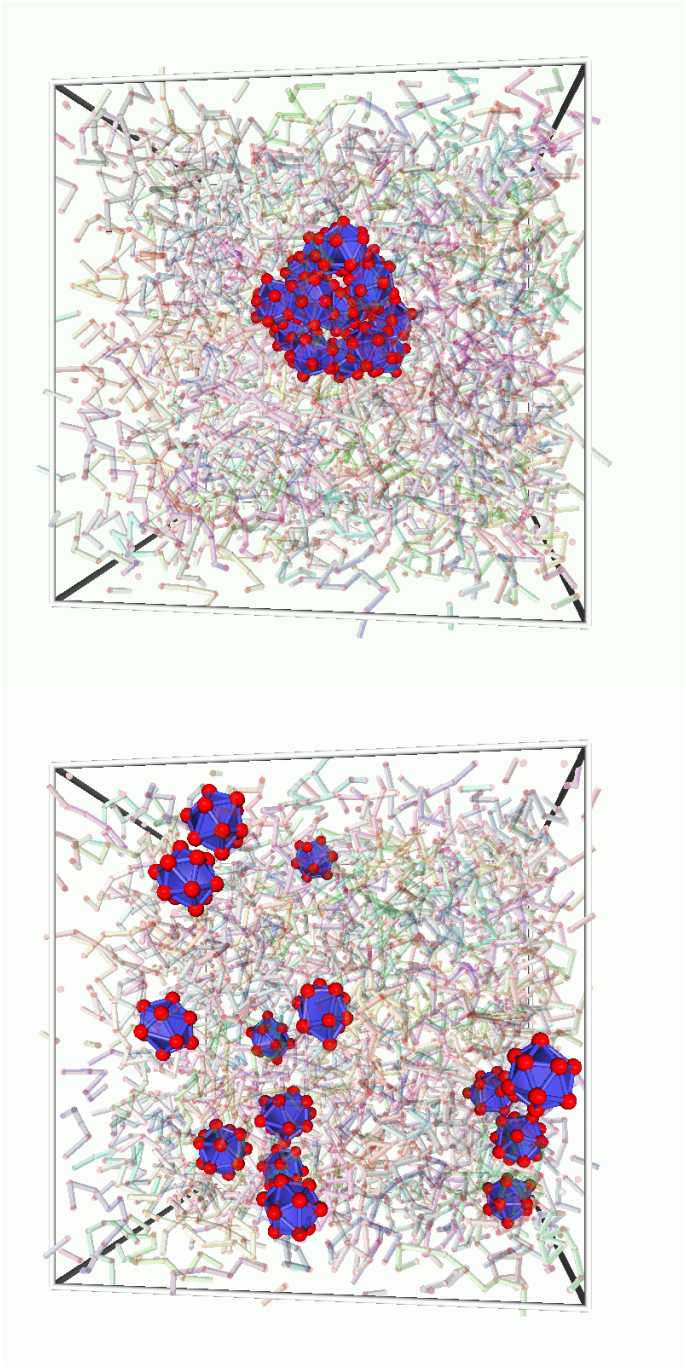

Figure 6: Simulation snapshots of for $T = 2.0$ and $\phi = 0.046$. (a) shows that the nanoparticles are clustered for a relatively weak interaction $\varepsilon_{\rm mp} = 1.0$. Similarly, (b) shows dispersion occurs for $\varepsilon_{\rm mp} = 1.5$. The chains are transparent to avoid obscuring the nanoparticles. The small spheres represent the locations of the Lennard-Jones force sites. [16]

small changes in the relative interactions between nanoparticles and polymer can cause dramatic qualitative changes in the structure of the system, which in turn must be reflected in the bulk properties of the material.

4.2 Relating material structure and properties

Development of new materials can be accelerated by understanding how the ultimate material properties are connected to the material structure. Thus it is desirable to connect how a rheological property like viscosity η varies as $\varepsilon_{\rm mp}$ changes, and hence reflects the degree of clustering. Viscosity is given by

$$\eta(\dot{\gamma}) = \langle P_{xy} \rangle / \dot{\gamma}, \tag{7}$$

where $\langle P_{xy} \rangle$ is the average of the component of the pressure tensor along the flow and gradient directions of the shear, and $\dot{\gamma}$ is the shear rate [16]. Ref. [16] evaluated η at fixed $\phi = 0.172$ and $\dot{\gamma} = 0.01$ — a low enough shear rate that the system is Newtonian [16]. Fig. 7(a) shows that η appears to approach nearly constant values at $\varepsilon_{\rm mp} = 1$ and 1.5, with a gradual crossover around $\varepsilon_{\rm mp} \approx 1.3$. In addition, $c_V^{\rm pp}$ of the sheared systems, shown in Fig. 7(b), indicates the crossover in clustering behavior occurs in the same range of $\varepsilon_{\rm mp}$ that η changes between asymptotic regimes. Thus η is sensitive to the state of particle clustering, and more sensitive to clustering than to variation of $\varepsilon_{\rm mp}$.

To take advantage of the fact that increased dispersion leads to an increase in viscosity, we also need to have some understanding of why this should be the case. In fact, hydrodynamic arguments would predict the opposite effect — that a large or extended rigid body embedded in a fluid results in a greater viscosity than a disperse collection of small rigid bodies [37]. But we must also consider the changes in the dynamics of the polymers near the surface of the nanoparticles, as discussed in the previous section. For attractive interactions, such as we have here, we know that relaxation times of surface monomers increase, corresponding to increase of the "local viscosity". For a well dispersed configuration, the amount of exposed nanoparticle surface grows linearly with the number of nanoparticles; if clustering occurs, the amount of exposed surface grows sub-linearly relative to the number of particles. Since we expect the changes in η are proportional to the amount of polymers that are in contact with the nanoparticles, then η should be larger for well-dispersed configurations than for clustered configurations.

A test of the expected correlation with the exposed surface area A is estimated by the fraction of nanoparticle force sites in contact with a chain (Fig. 7(c)). There is a large change in A in the same range as the large changes in η. However, we note that that the regions where A and η significantly change do not match precisely. This may be an indication that less pronounced hydrodynamic effects do play a role. Some progress in accounting for hydrodynamic effects on viscosity in a system with a single nanoparticle

Soft Materials: Structure and Dynamics pp. 107-124
Eds.: J. R. Dutcher and A. G. Marangoni (2004)

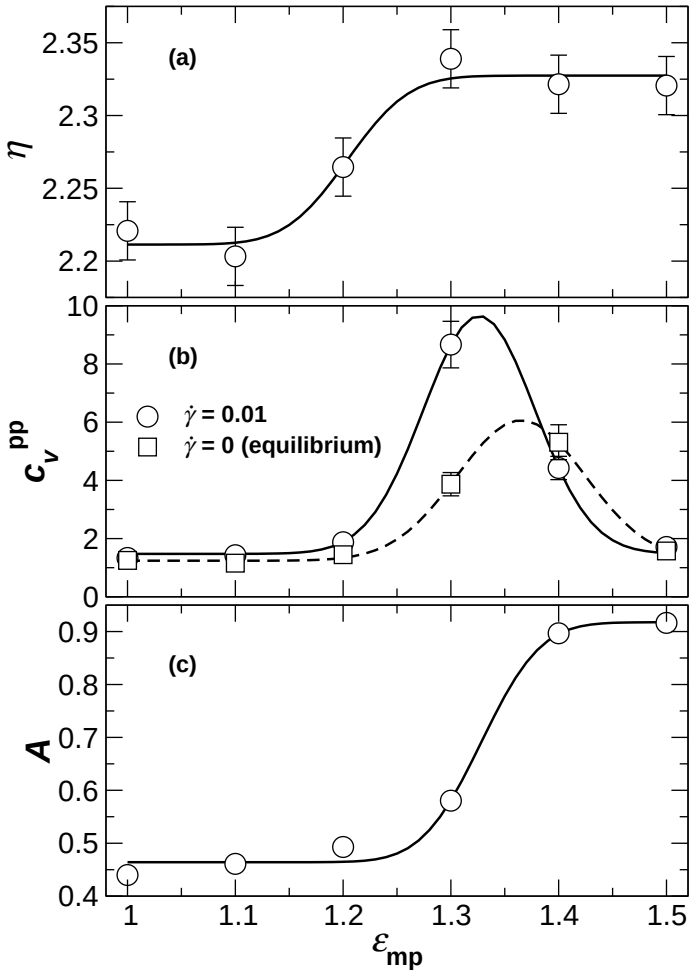

Figure 7: (a) Viscosity η as a function of $\varepsilon_{\rm mp}$ at fixed $T = 2.0$ and $\phi = 0.172$. (b) Specific heat calculated for the sheared configurations (circles, solid line) and equilibrium configurations (squares, broken line). Note the shift in the maximum, and its location compared with the crossover in the behavior of η. (c) The fraction of nanoparticle force sites in contact with a polymer, an estimate of the exposed surface area A. The lines serve only as guides to the eye. Figure reproduced from ref. [16].

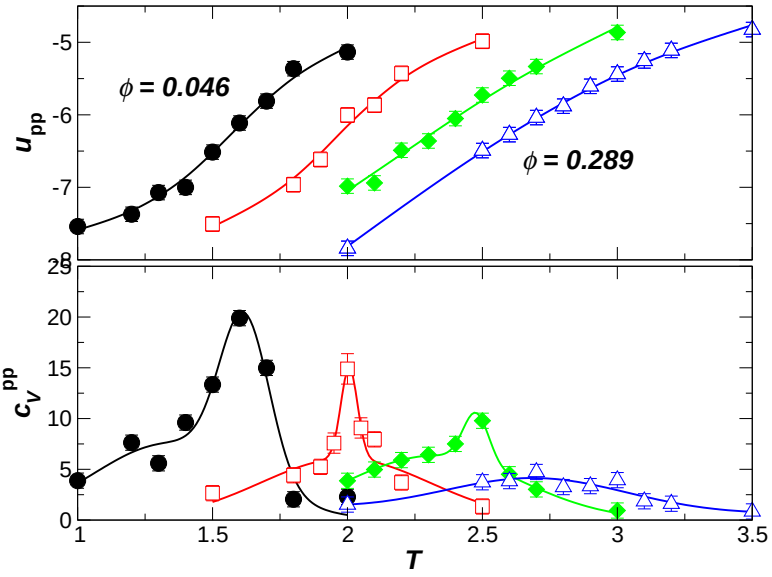

Figure 8: (a) Potential energy $u_{\rm pp}$ and (b) specific heat $c_V^{\rm pp}$ as a function of T for loadings $\phi = 0.046$ ($\circ$), 0.094 ($\Box$), 0.172 ($\diamond$), and 0.289 ($\triangle$). Nanoparticles are clustered for low $u_{\rm pp}$, and the approximate boundary between clustered and dispersed states is given by the maximum in $c_V^{\rm pp}$. The lines are only a guide to the eye. [16]

has been made [21], but these results do not account for changes due to clustering in non-dilute nanoparticle composites.

4.3 Physical mechanism controlling clustering

In this subsection, we discuss the possible physical process though which particle clustering occurs. There are a variety of possible mechanisms, the most obvious of which is that particles cluster via ordinary phase separation, as in a binary mixture. Phase separation of this type is first order, and so it is expected that $u_{\rm pp}$ and $c_V^{\rm pp}$ exhibit a discontinuity at the transition line, provided we do not follow a path through the critical point. We can see that in Fig. 5, the crossover from dispersed to clustered states appears to occur through a continuous process. At first glance, this would argue against phase separation, but we must consider that, because of the finite size of the system, we expect rounding of the transition [38]. So while these results are not inconsistent with phase separation, we need further evidence to make a compelling case for, or against phase separation.

To obtain such evidence, the system was cooled from the dispersed to the clustered

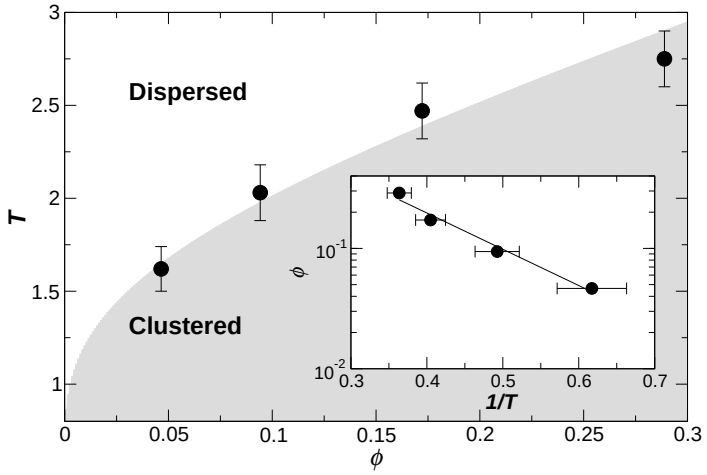

Figure 9: (a) The "clustering diagram" of the nanoparticles, as a function of T and ϕ. The boundary of the shaded region is determined by fitting the points using equation 8, shown in the inset. Figure reproduced from ref. [16].

phase for several different ϕ at fixed $\varepsilon_{\rm mp} = 1.3$. In doing so, ref. [16] estimated the approximate phase boundary, thereby determining if the behavior of the specific heat matches the expectations for phase separation — namely that $c_V^{\rm pp}$ should be increasing towards divergence as we approach the critical point of the transition. In Fig. 8 we show the behavior of $u_{\rm pp}$ and $c_V^{\rm pp}$ as a function of T for several loadings. The peak in $c_V^{\rm pp}$ facilitates identification of a clustering boundary. The temperature T^* of the boundary between clustered and dispersed states is approximated by the location of the maximum in $c_V^{\rm pp}$. Fig. 9 shows the boundary is positively sloped, indicating that clustering occurs for large ϕ and low T. If the clustering mechanism were analogous to binary phase separation, the critical point must be at some $\phi > 0.3$, since the boundary is positively sloped to that ϕ. Hence, the maximum value of $c_V^{\rm pp}$ should be increasing as ϕ increases towards a possible critical point. However, Fig. 8(b) shows that the amplitude of the peak in $c_V^{\rm pp}$ *decreases* and becomes broader as we increase ϕ. Hence the behavior of $c_V^{\rm pp}$ appears to be contrary to our expectations for phase separation.

If nanoparticle clustering is not governed by a phase separation process, then what is the controlling mechanism? The decrease in the amplitude of the $c_V^{\rm pp}$ peak with increasing ϕ is consistent with the predicted behavior for an associating system [39, 40]. The model of equilibrium polymerization [40] also predicts that the loci of specific heat

maxima should shift location according to

$$\phi \sim \exp(-E_1/T^*). \tag{8}$$

Within the limits of uncertainty in the data, the clustering boundary shown in Fig. 9 can be described by equation 8. These findings suggest that the clustering transition in this system, and presumably in many similar real nanocomposite systems characterized by short-range, van der waals-type interactions , is controlled by the same mechanism as simple associating systems. This observation provides a framework for rationalizing the behavior of many nanoparticle systems, which should in turn aid in the control of dispersion and nanocomposite properties.

5 CONCLUSION

In this chapter, we have reviewed the results of molecular dynamics simulations of a coarse-grained model of a nanoparticle-filled polymer melt. These simulations provide insight into how polymer-nanoparticle interactions can affect structural, dynamical, thermodynamic, and rheological properties of the matrix polymer. The scientific understanding obtained by our results can be used to guide the engineering of polymer nanocomposites through the manipulation of the interfacial interactions between the organic and inorganic components. For more detailed insight on a specific polymer-nanoparticle composite, atomistic simulations with more realistic force fields are necessary. However, such simulations alone cannot be performed for large systems due to the computational cost of including such a high level of detail, and thus multiscale approaches are needed, whereby electronic and atomistic detail obtained from a combination of *ab initio* and atomistic simulation techniques are fed upwards to parameterize models for coarse-grained simulations such as those described here [41]. In turn, output from the coarse-grained simulations can be fed into, e.g., field theoretic simulations for the prediction of microstructures resulting from thermodynamic immiscibility in nanoparticle-filled polymers and blends [42–44], and these microstructures can be fed into macroscopic models for calculation of bulk properties like conductivity and modulus [45].

There is increasing evidence that nanoparticle shape can play a large role in dictating properties of the matrix in which the nanoparticles are dispersed. Clay platelets, for example, can induce different degrees of changes than spherically symmetric nanoparticles composed of the same material [46–48]. Recent simulations of tethered nanoparticles, in which nanoparticles are not dispersed freely in a matrix but rather are combined with polymeric tethers through covalent bonding of the tethers to strategic locations on the nanoparticle surface, indeed demonstrate the important of nanoparticle shape in controlling local nanoparticle packing when nanoparticles and tethers are immiscible [49].

Functionalization of nanoparticles and inorganic nanostructured molecules by cross-linking polymers is another approach to engineering polymer/nanoparticle nanocomposites [50, 51]. Here, too, simulations can provide insight via a systematic investigation of the local structure and mechanical properties and how they depend on such characteristics as polymer molecular weight, stiffness, and functionality of the nanoparticle [52].

References

[1] MRS Bulletin, May 2001 issue.
[2] R.A. Vaia and E.P. Giannelis, MRS Bulletin **26**, 394 (2001).
[3] R.A. Vaia and E.P. Giannelis (eds.). *Polymer Nanocomposites* (American Chemical Society, Washington, 2001).
[4] E.P. Giannelis, Adv. Mater. **8**, 29 (1996).
[5] T. Kashiwagi, E. Grulke,J. Hilding, R. Harris, W. Awad, J. Douglas, Macromolecules **23**, 761 (2002).
[6] Y. Tang, et al., Polymer Int. **52**, 1396 (2003).
[7] C.B. Murray, C.R. Kagan, M.G. Bawendi, Annu. Rev. Mater. Sci. **30**, 545 (2000).
[8] B.D. Busbee, S.O. Obare, C.J. Murphy, Adv. Mater. **15**, 414 (2003).
[9] Y.G. Sun and Y.N. Xia, Science **298**, 2176 (2002).
[10] N. Pinna, K. Weiss, J. Urban, M.-P. Pileni,. Adv. Mater. **13**, 261 (2001).
[11] F.M.V. Kooij, K. Kassapidou, H.N.W. Lekkerkerker, Nature **406**, 868 (2000).
[12] L. Manna, D.J. Milliron, A. Meisel, E.C. Scher, P.A. Alivisatos, Nature Mater. **2**, 382 (2003).
[13] R. Jin, Y. Cao, C.A. Mirkin, K.L. Kelly, G.C. Schatz, J.G. Zheng, Science **294**, 1901 (2001).
[14] F.W. Starr, T.B. Schrøder, and S.C. Glotzer, Phys. Rev. E **64**, 021802 (2001)
[15] F.W. Starr, T.B. Schrøder, and S.C. Glotzer, Phys. Rev. E **64**, Macromolecules **35**, 4481 (2002).
[16] F.W. Starr, J.F. Douglas, and S.C. Glotzer, J. Chem. Phys. **119**, 1777 (2003).
[17] M. Vacatello, Macromolecules **34**, 1946 (2001).
[18] M. Vacatello, Macromolecules **35**, 8191 (2002).
[19] M. Vacatello, Macromol. Theor. Simul. **11**, 757 (2002).
[20] S. Salaniwal, S.K. Kumar, and J.F. Douglas, Phys. Rev. Lett. **89**, 258301 (2002)
[21] G.D. Smith, D. Bedrov, L. Li, and O. Byutner, J. Chem. Phys. **117**, 9478 (2002).
[22] J.S. Smith, D. Bedrov, G.D., Compos. Sci. Technol. **63**, 1599 (2003).
[23] D. Brown, P. Mélé, S. Marceau, and N.D. Albérola, Macromolecules **36**, 1395 (2003).
[24] D. Gersappe, Phys. Rev. Lett. **89**, 058301 (2002).
[25] D.H. Cole, K.R. Shull, P. Baldo, and L. Rehn, Macromolecules **32**, 771 (1999); F. Carusoa and H. Mohwald, Langmuir **15**, 8276 (1999); K.V. Sarathy, K.S. Narayan, J. Kim, and J.O. White, Chem. Phys. Lett. **318**, 543 (2000).
[26] K.A. Barnes, A. Karim, J.F. Douglas, A.I. Nakatani, H. Gruell, and E.J Amis, Macro-

molecules **33**, 4177 (2000); B. McCarthy, J.N. Coleman, S.A. Curran, A.B. Dalton, A.P. Davey, Z. Konya, A. Fonseca, J.B. Nagy, and W.J. Blau, J. Mater. Sci. Lett. **19**, 2239 (2000).

[27] R.B. Bird, C.F. Curtiss, R.C. Armstrong, and O. Hassager, *Dynamics of Polymeric Liquids: Kinetic Theory, Vol. 2*. (John Wiley and Sons, New York, 1987).

[28] G.S. Grest and K. Kremer, *Phys. Rev. A* **33**, 3628 (1986).

[29] J.W. Rudisill and P.T. Cummings, Rheologica Acta **30**, 33 (1991).

[30] S.K. Kumar, M. Vacatello, and D.Y. Yoon, J. Chem. Phys. **89**, 5206 (1989).

[31] S.K. Kumar, M. Vacatello, and D.Y. Yoon, Macromolecules **23**, 2189 (1990).

[32] J.-S. Wang, and K. Binder, J. Phys. I France **1**, 1583 (1991).

[33] C. Mischler, J. Baschnagel, and K. Binder, Adv. Colloid Interfac. **94**, 197 (2001), and references therein.

[34] G.D. Smith, D. Bedrov, and O. Borodin, Phys. Rev. Lett. **90**, 226103 (2003).

[35] P.G. Debenedetti, *Metastable Liquids* (Princeton Univ. Press, Princeton, 1996).

[36] D.A. Savin, J. Pyun, G.D. Patterson, T. Kowalewski, K. Matyjaszewski, J. Poly. Sci. Poly. Phys. **40**, 2667 (2002).

[37] J. Bicerano, J.F. Douglas, and D.A. Brune, Rev. Macromol. Chem. Phys. **C39**, 561 (1999).

[38] K. Binder, Rep. Prog. Phys. **50**, 783 (1987).

[39] S.C. Greer, Ann. Rev. Phys. Chem. **53**, 173 (2002).

[40] J. Dudowicz, K.F. Freed, and J.F. Douglas, J. Chem. Phys. **111**, 7116 (1999); J. Chem. Phys. **112**, 1002 (2000).

[41] S.C. Glotzer and W. Paul, Annu. Rev. Mater. Res., 32, 401-436 (2002).

[42] B.P. Lee, J.F. Douglas, and S.C. Glotzer, Phys. Rev. E 60, 5812 (1999).

[43] V.V. Ginzburg and A.C. Balazs, Macromolecules **32**, 5681. (1999)

[44] V.V. Ginzburg, C. Singh, and A.C. Balazs, Macromolecules **33**, 1089 (2000).

[45] F.W. Starr and S.C. Glotzer, Materials Research Society Fall '00 Proceedings: Filled and Nanocomposite Polymer Materials, 661, 1 (2001).

[46] G. Schmidt and M.M. Malwitz, Curr. Opin. Colloid and Int. **8**, 103 (2003).

[47] J.J. Luo and I.M. Daniel, Compos. Sci. Technol. **63**, 1607 (2003).

[48] T.D. Fornes and D.R. Paul, Polymer **44**, 4993 (2003).

[49] Z.L. Zhang, M.A. Horsch, M.H. Lamm and S.C. Glotzer, Nano Letters, in press.

[50] C.L. Soles, E.K. Lin, W.L. Wu, C. Zhang, and R.M. Laine, Organic/Inorganic Hybrid Materials; Materials Research Society: Warrendale, Pa., 2000; Vol. 628.

[51] J. Choi, A.F. Yee, R.M. Laine, Macrocolecules **36** 5666 (2003).

[52] M.H. Lamm, T. Chen and S.C. Glotzer, Nano Letters, 3(8), 989 (2003).